

Prioritising COVID-19 vaccination in changing social and epidemiological landscapes

Peter Jentsch^{1,2}, Madhur Anand¹, and Chris T. Bauch^{2,*}

¹Department of Applied Mathematics, University of Waterloo, Waterloo, Ontario, Canada; ²School of Environmental Sciences, University of Guelph, Guelph, Ontario, Canada; *cbauch@uwaterloo.ca

1 Summary

2 **Background.** During the COVID-19 pandemic, authorities must decide which groups to prioritise for
3 vaccination. These decision will occur in a constantly shifting social-epidemiological landscape where
4 the success of large-scale non-pharmaceutical interventions (NPIs) like physical distancing requires broad
5 population acceptance.

6 **Methods.** We developed a coupled social-epidemiological model of SARS-CoV-2 transmission. Schools
7 and workplaces are closed and re-opened based on reported cases. We used evolutionary game theory and
8 mobility data to model individual adherence to NPIs. We explored the impact of vaccinating 60+ year-olds
9 first; <20 year-olds first; uniformly by age; and a novel contact-based strategy. The last three strategies
10 interrupt transmission while the first targets a vulnerable group. Vaccination rates ranged from 0.5% to
11 4.5% of the population per week, beginning in January or July 2021.

12 **Findings.** Case notifications, NPI adherence, and lockdown periods undergo successive waves during the
13 simulated pandemic. Vaccination reduces median deaths by 32% – 77% (22% – 63%) for January (July)
14 availability, depending on the scenario. Vaccinating 60+ year-olds first prevents more deaths (up to 8%
15 more) than transmission-interrupting strategies for January vaccine availability across most parameter
16 regimes. In contrast, transmission-interrupting strategies prevent up to 33% more deaths than vaccinating
17 60+ year-olds first for July availability, due to higher levels of natural immunity by that time. Sensitivity
18 analysis supports the findings.

19 **Interpretation.** Further research is urgently needed to determine which populations can benefit from using
20 SARS-CoV-2 vaccines to interrupt transmission.

21 **Funding.** Ontario Ministry of Colleges and Universities.
22

23 Research in context

24 **Evidence before this study.** Whether to vaccinate individuals who cause the most transmission or those
25 who are at highest risk of death is relevant to prioritizing COVID-19 vaccination. We searched PubMed and
26 medRxiv for the terms COVID19, vaccin*, model, and priorit* up to September 24, 2020, with no date or
27 language restrictions. We identified 4 papers on mathematical models of COVID-19 vaccine prioritization
28 that explored the conditions under which different age groups should be vaccinated first. We did not find
29 any coupled social-epidemiological models that capture feedback between social dynamics and epidemic
30 trajectories.

31 **Added value of this study.** The dynamic interaction between SARS-CoV-2 epidemics and the population
32 response through scalable non-pharmaceutical interventions will continue to play a large role in the course
33 of the pandemic, both before and after vaccines become available. Hence, social-epidemiological models
34 may be useful. Our social-epidemiological model identifies the conditions under which COVID-19 deaths
35 can be reduced most effectively by prioritizing older individuals first, versus other strategies designed to
36 interrupt transmission. We explore how the best vaccination strategy varies depending on a wide range
37 of socio-epidemiological and vaccine program parameters. We identify clear and interpretable conditions
38 under which using COVID-19 vaccines to interrupt transmission can reduce mortality most effectively.

39 **Implications of all the available evidence.** Seroprevalence surveys before the onset of vaccination could
40 measure population-level SARS-CoV-2 immunity. In populations where seropositivity is high due to

41 previous waves, vaccinating to interrupt transmission may reduce deaths more effectively than targeting
42 older individuals. More research is urgently required to evaluate how to prioritise vaccination in populations
43 that have experienced one or more waves of COVID-19.

44 Introduction

45 The COVID-19 pandemic has imposed a massive global health burden as waves of infection to move
46 through populations around the world (1). Both empirical analyses and mathematical models conclude
47 that non-pharmaceutical interventions (NPIs) are effective in reducing COVID-19 case incidence (2–4).
48 However, pharmaceutical interventions are highly desirable given the socio-economic costs of lockdown
49 and physical distancing. Hence, dozens of vaccines are in development (5), and model-based analyses are
50 exploring the question of which groups should get the COVID-19 vaccine first (6, 7).

51 When vaccines become available, we will face a very different epidemiological landscape from the early
52 pandemic. Many populations will already have experienced one or more waves of COVID-19. As a result
53 of natural immunity, the effective reproduction number R_{eff} (the average number of secondary infections
54 produced per infected person) will be reduced from its original value of approximately $R_0 = 2.2$ in the
55 absence of pre-existing immunity (8). Epidemiological theory tells us that as R (or R_0) decline toward 1,
56 the indirect benefits of transmission-blocking vaccines become stronger. For instance, if $R_{eff} \approx 1.5$, such as
57 for seasonal influenza, only an estimated 33% percent of the population needs immunity for transmission
58 to die out in a homogeneously population (9, 10). This effect was evidenced by the strong suppression of
59 influenza incidence in Australia in Spring 2020 due to NPIs targeted against COVID-19 (11).

60 This effect has stimulated a literature comparing the effects of vaccinating subpopulations that are
61 responsible for most transmission, to vaccinating subpopulations that are vulnerable to serious complications
62 from the infection but exhibit weaker immune responses to the vaccine (10, 12, 13). Natural population
63 immunity to SARS-CoV-2 will likely continue to rise for many populations on account of further infection
64 waves. Given these likely changes to the epidemiological landscape before the vaccine becomes available, we
65 suggest this question is worthy of investigation in the context of COVID-19.

66 The social landscape will also look very different when vaccines become available and this aspect is
67 crucial to understanding the pandemic. Scalable non-pharmaceutical interventions (NPIs) like physical
68 distancing, hand-washing and masks are often one of the few available interventions when a novel pathogen
69 emerges. Flattening the COVID-19 epidemic curve was possible due to a sufficient response by populations
70 willing to adhere to public health recommendations. Therefore, pandemic waves are not simply imposed
71 on populations, but rather are also a creation of the population response to the pathogen (14?). Thus,
72 pandemics caused by novel pathogens can be characterized as coupled socio-epidemiological systems
73 exhibiting two-way feedback between disease dynamics and behavioural dynamics.

74 Approaches to modelling coupled social-epidemiological dynamics vary (15–19). Some previous models
75 have used evolutionary game theory (EGT) to model this two-way feedback in a variety of coupled human-
76 environment systems (14, 20–25). EGT is relevant to population adherence to NPIs since it captures how
77 individuals learn social behaviours from one another while weighting personal risks and benefits of different
78 choices. In this framework, individuals who do not adopt NPIs can ‘free-ride’ on the benefits of reduced
79 transmission generated by individuals who do (15).

80 Here, our objective is to compare projected COVID-19 mortality reductions under four strategies for
81 the prioritization of COVID-19 vaccines: elderly first, children first, uniform allocation, and a novel
82 strategy based on the contact structure of the population. We use an age-structured model of SARS-CoV-2
83 transmission, including an evolutionary game theory submodel for population adherence to NPIs fitted
84 to mobility data. We use extensive scenario and sensitivity analysis to identify how strategy effectiveness
85 responds to possible changes in the social-epidemiological landscape that may occur both before and vaccines
86 are available.

87 **Model Overview**

88 **Structure and parameterisation.** We developed an age-structured SEAIR model (Susceptible, Exposed,
89 Asymptomatic Infectious, Symptomatic Infectious, Removed) with ages in 5-year increments. Upon infection,
90 individuals enter an exposed category where they are infected but not yet infectious. After the exposed
91 stage, individuals become either symptomatically or asymptotically infectious, and enter the Removed
92 compartment when their infectious period ends. Since our focus was on vaccination, we did not model
93 testing or contact tracing. Transmission occurred through an age-specific contact matrix, susceptibility to
94 infection was age-specific, and we included seasonality due to changes in the contact patterns throughout
95 the year. Details of our model structure, parameterization, and sources appear in the Supplementary
96 Appendix (Methods and Table S1). The model was parameterized with data from Ontario, Canada.

97 Both schools and workplaces were closed when the proportion of ascertained active cases surpassed
98 50%, 100%, 150%, 200%, or 250% of the level that sparked shutdown during the first wave, and were
99 re-opened again when cases fell below that threshold. For our evolutionary game model of adherence to
100 NPIs like mask use and physical distancing, we assumed that individuals weigh the cost of practicing NPIs
101 imposed by reduced socialization, money spent on masks, *etc*, against the cost of not practicing NPIs and
102 thereby experiencing an increased perceived risk of infection according to the prevalence of ascertained cases.
103 Individuals sample other individuals and may switch between adherence and non-adherence to NPIs as a
104 result, with a probability proportional to the difference in these costs. Both school and workplace closure
105 and the proportion of the population practicing NPIs impact transmission according to their respective
106 intervention efficacy.

107 We used a Bayesian particle filtering approach to fit the model to case notification and mobility data from
108 Ontario (see Supplementary Appendix for detailed methods and literature sources). We performed particle
109 filtering on all social and epidemiological model parameters that could not be fixed at point estimates from
110 the published literature, such as the ascertainment rates for each age group, the basic reproduction number
111 R_0 , and the social submodel parameters. Posterior distributions for fitted parameters appear in Figure
112 S1. The temporal curve describing contacts under workplace closing and opening were also fit to mobility
113 data. Mobility data specific to school closure does not exist, so we assumed that outside of the normal
114 school breaks (*e.g.* summer holiday), schools exhibit similar temporal curves describing opening and closing
115 as workplace do. We used published COVID-19 case fatality rates to determine number of deaths by age
116 group based on the predicted incident cases by age group. Posterior distribution of model fits to age-specific
117 cumulative cases appear in Figure S2, and posterior model time series fits appear in Figure 1.

118 **Vaccine scenarios.** We considered two different dates for the onset of vaccination: 1 January 2021 and 1
119 July 2021. These correspond to the dates at which vaccine-derived immunity in the vaccine is achieved,
120 hence the actual administration of a two-dose course would start approximately two weeks before these
121 dates. We considered that it was possible to vaccinate 0.5%, 1.5%, 2.5%, 3, 5%, or 4.5% of the population
122 per week. Our baseline scenario assumed an all-or-none vaccine with 90% efficacy against both infection
123 and transmission.

124 The “oldest first” strategy administers the vaccine to individuals 60 years of age or older first. Re-
125 vaccination is only possible one more time if the vaccine did not “take” the first time. After all individuals
126 in this group are vaccinated, the vaccine is administered uniformly to other ages. The “youngest first”
127 strategy is similar, except it administers the vaccine to individuals younger than 20 years of age first. The
128 “uniform” strategy administers vaccine to all individuals regardless of their age from the very beginning.
129 The “contact-based” strategy allocates vaccines according to the leading eigenvector of the next-generation
130 matrix (Supplementary Appendix). This tends to prioritise ages 15-19 primarily, 20-59 secondarily, and the
131 least in older or younger ages (Figure S3). The “oldest first” strategy targets a vulnerable age group while
132 the other three strategies are designed to interrupt transmission. We also explored an optimal strategy that
133 seeks to optimize age-specific vaccine coverage to minimize the number of deaths over five years from the
134 beginning of the epidemic. This used local optimization from each of the aforementioned strategies (see

135 Supplementary Appendix).

136 **Sensitivity analysis.** Sensitivity analysis was conducted for eight scenarios corresponding to: (1) constant
137 physical distancing (instead of using evolutionary game theory to describe population behaviour), (2)
138 increased efficacy of physical distancing (+0.2) after the first wave on account of more widespread mask
139 use, (3) a higher basic reproduction number, $R_0 = 2.3$, compared to our baseline fit (4) 50% vaccine
140 efficacy in the elderly and 90% for other ages, (5) 50% vaccine efficacy in everyone, (6) no seasonality in the
141 transmission rate, (7) constant susceptibility across all ages, and (8) vaccinating only individuals without
142 pre-existing immunity.

143 **Role of the funding source.** The funder of the study had no role in study design, data collection, data
144 analysis, data interpretation, or writing of the manuscript. The corresponding author had full access to all
145 the data in the study and had final responsibility for the decision to submit for publication.

146 Results

147 **Temporal dynamics before and after vaccination.** The Google mobility data used as a proxy for adherence
148 to NPIs closely mirrors the COVID-19 case notification data over the Spring/Summer 2020 time period
149 used for fitting (Figure 1, open circles). Since NPIs can significantly reduce SARS-CoV-2 transmission
150 (2, 3) and a heightened perception of COVID-19 infection risk simulates the adoption of NPIs (26), this
151 exemplifies a social-epidemiological dynamic. Moreover, the fit of the social submodel to the mobility data
152 is as good as the fit of the epidemic submodel to the case notification (Figure 1). The social and epidemic
153 submodels have a similar number of parameters (Supplementary Appendix), and the social model consists
154 of a single equation, in contrast to the dozens of equations used for our age-structured compartmental
155 model. This shows how modelling population behaviour during a pandemic can be accomplished with
156 relatively simple mechanistic models.

157 Extrapolating beyond the fitting time window, the model predicts several pandemic waves from late Fall
158 2020 onward, not only with respect to COVID-19 cases (Figure 2A) but also population adherence to NPIs
159 (Figure 2B) and periods of school and workplace shutdown (Figure 2C). The unfolding of the pandemic
160 if the vaccine becomes available in July 2021 (vertical dashed line) and 4.5% of the population can be
161 vaccinated per week depends upon the vaccination strategy. The oldest first strategy (blue) results in a
162 large pandemic wave in late December 2021. The youngest first (orange) and uniform (green) strategies
163 result in a smaller wave in late March 2022. The contact-based strategy (red) avoids a Fall 2021/Winter
164 2022 wave altogether. In contrast, vaccinating 4.5% of the population per week starting in January hastens
165 the end of the Fall 2020/Winter 2021 wave and prevents subsequent pandemic waves (Figure S4).

166 During each wave, the percentage of individuals with natural immunity rises (Figure 2D). Once the
167 vaccine becomes available, total population immunity from the vaccine or from infection rises most slowly
168 under the youngest first strategy. However, we note that strategy effectiveness is also a function of the
169 contract structure of the population.

170 **Relative mortality reductions under the vaccine strategies.** We determined the cumulative number of
171 deaths over the duration of the pandemic for each strategy across a range of vaccine availability dates
172 and vaccination rates. Broadly speaking, if the vaccine becomes available in January 2021, the oldest first
173 strategy reduces mortality the most. But if the vaccine becomes available in July 2021, one of the other
174 three transmission-interrupting strategies is most effective (Figures 3, 4).

175 For our baseline assumption where schools and business close when active cases reach $T = 200\%$ of the
176 numbers that sparked shutdown during the first wave, and for a January vaccine availability, the oldest
177 first strategy prevents the most deaths except for a very low vaccination rate ($\psi_0 = 0.5\%$ of the population
178 vaccinated per week (Figure 3a)). But for July vaccine availability, the contact-based strategy does best,
179 except when $\psi_0 = 0.5\%$, where oldest first is best (Figure 3B). However, all strategies perform similarly at
180 high vaccination rates because population immunization occurs fast enough to prevent a Fall 2021/Winter

181 2022 wave. Across a broader range of T values from 50% to 250%, the same patterns generally hold (Figure
182 S5,6). The violin plots show a dominant lobe and a smaller secondary lobe, on account of the fact that
183 some parameter combinations generate more pandemic waves than others (Figure 3). This effect is more
184 apparent when $T = 250\%$ (Figure S5,6).

185 These results are also confirmed by a higher resolution parameter plane showing the best strategy as
186 a function of T and ψ_0 (Figure 4; the best strategy in this case is defined as the strategy that reduced
187 mortality the most across the largest number of model realizations). For January availability, the oldest
188 first strategy is most effective if $\psi_0 \gtrsim 1.5\%$, but for July availability, the contact-based strategy is best for
189 low vaccination rates and youngest first is best for medium to high vaccination rates, unless T is also high,
190 in which case uniform is best.

191 The optimized strategy always does best, by definition (Figure S5,6), but it can be instructive to study
192 how the optimized strategy allocates vaccines among the age groups. We observe that for strict shutdown
193 thresholds (small T), the optimal strategy allocates vaccines mostly to the 5-19 age group, secondly to
194 35-44, and thirdly to 70+. As the shutdown thresholds become more lenient, more vaccine is allocated to
195 70+ (Figure S7).

196 We emphasise that we are reporting percent change in mortality compared to the case of no vaccine
197 being available. Therefore, the total reduction in number of COVID-19 deaths for January availability is
198 much higher than for July availability on account of intervening pandemic waves.

199 **Role of R_0 and herd immunity.** Studying the role of the basic reproduction number, R_0 (9), and the
200 immunity profile of the population helps to explain these results. Our inferred value was $R_0 \approx 1.8$. As
201 R_0 is increased from 1.5 to 2.5 we observe that the vaccine becomes less effective in reducing mortality
202 across all strategies, as expected (Figure 5). For January availability, oldest first does best across all R_0
203 values (Figure 5A). For July availability, oldest first does worst when R_0 is small, but improves relative
204 to the other strategies as R_0 increases (Figure 5B). This occurs because the indirect protection (herd
205 immunity) offered by transmission-blocking vaccines are strongest when R_0 is small. In populations with
206 strong age-assortative mixing (27), the indirect benefits of vaccination are therefore “wasted” if vaccination
207 is first concentrated in specific age groups before being extended to the rest of the population. When R_0 is
208 larger, however, the indirect protection of vaccine-generated herd immunity is weaker (9) and so the benefit
209 of using vaccines to interrupt transmission is reduced.

210 Frequency histograms for each strategy of the percentage of the population with natural immunity
211 at the start of the vaccine program, for the simulations where that particular strategy worked best, tell
212 a similar story (Figure 6). In simulations where the oldest first strategy does best, the percentage of
213 the population with natural immunity tends to be low. This is expected, since indirect protection from
214 vaccines is weak when few people have immunity (Figure 6A). But in simulations where one of the three
215 transmission-interrupting strategies do best, more simulations exhibited a high level of natural population
216 immunity at the start of vaccination (Figure 6B-D).

217 **Sensitivity analysis results.** The relative advantage of transmission-interrupting strategies for July vaccine
218 availability generally either remained the same or improved across the nine alternative scenarios described
219 in the Model Overview section.

220 We explored a model variant where population adherence to NPIs is constant over the course of the
221 pandemic, although dynamic shutdown of schools and workplaces still occurred. We observed that the
222 youngest first strategy did best for both January and July vaccine availability, except for strict shutdown
223 thresholds $T \lesssim 75\%$ in which case the oldest first strategy did best (and also for January availability,
224 with high T and ψ_0 , Figure S8). Youngest first performed even better in a model variant where infection
225 susceptibility is constant across ages (Figure S9). In the absence of seasonality, the youngest first strategy
226 almost always does best for both January and July availability (Figure S10). Similarly, when vaccine efficacy
227 is 50% in older individuals and 90% for everyone else, the transmission-interrupting strategies generally do
228 best for both January and July availability (Figure S11).

229 Several of the sensitivity analysis scenarios produced similar outcomes to the baseline scenario, with
230 oldest first generally doing best for January availability, and one of the transmission-interrupting strategies
231 (usually, youngest first) doing best for July availability. These scenarios were: increased efficacy of NPIs in
232 the second wave to account for more widespread use of masks (Figure S12); $R_0 = 2.3$ (Figure S13); 50%
233 vaccine efficacy for everyone (Figure S14), and when individuals are tested for seropositivity before being
234 administered a vaccine (Figure S15).

235 Discussion

236 Our social-epidemiological model suggests that if a COVID-19 vaccine becomes available later in the
237 pandemic, using SARS-CoV-2 vaccines to interrupt transmission might reduce COVID-19 mortality more
238 effectively than using the vaccines to target those 60+ years of age, in many populations. This finding
239 was robust under structural and univariate sensitivity analyses, including model variants with a more
240 conventional structure lacking social dynamics or seasonality.

241 These results are driven by the fact that the vaccine may only become available after populations have
242 had one or more waves of immunizing infections. As a result, the effective reproduction number could be
243 significantly lower than the basic reproduction number $R_0 \approx 2.3$ which applies in susceptible populations.
244 In this regime, vaccines have a disproportionately large effect in terms of generating herd immunity (9).
245 This effect has also been observed in influenza, both in theoretical models and in recent experience with
246 the Spring wave of COVID-19 in Australia (10, 11). In the later case, NPIs interrupted SARS-CoV-2
247 transmission enough to flatten the curve for COVID-19 with $R_0 \approx 2.3$, but for influenza with $R_0 \approx 1.5$,
248 NPIs strongly suppressed influenza activity country-wide. In a population with several waves of COVID-19,
249 R_{eff} may come sufficiently close to 1 that immunizing to interrupt transmission will be the most effective
250 strategy to reduce mortality.

251 We opted for a coupled social-epidemiological model on account of the importance of feedback between
252 population behaviour and disease dynamics for the control of COVID-19 in the absence of preventive
253 pharmaceutical interventions. Our model generated significantly different projections in our sensitivity
254 analysis where population behaviour was assumed constant, which is similar to conventional approaches to
255 transmission modelling. Our social submodel is less complicated than the epidemic submodel and despite
256 this, the coupled social-epidemiological model fitted population-level behaviour as readily as it fitted the
257 epidemic curve. Predicting behaviour is fraught with uncertainty, but so is predicting an epidemic curve.
258 Given this, we suggest a role for more widespread use of social-epidemiological models in efforts model
259 NPIs during pandemics. We also note that the population-level behaviour and the epidemic curve closely
260 mirrored each other (Figure 1). This may reflect convergence of social-environment dynamics, as has been
261 predicted for strongly coupled systems (28).

262 Our model made simplifying assumptions that could impact its predictions. We did not stratify the
263 population by risk factors such as co-morbidities, and we did not consider outcomes such as hospitalizations
264 and ICU admissions. The model was parameterised with data from Ontario, Canada. The projected impact
265 of the four vaccine strategies may differ in settings with different epidemiological or social characteristics. At
266 the same time, we note that many populations around the world experienced a Spring 2020 wave, as Ontario
267 did. And, Ontario intensive care bed capacity resembles that of many other European countries (29). We
268 did not account for the potential role of outbreaks in long-term care facilities with high concentrations of
269 vulnerable individuals. Finally, we used baseline changes to time spent at retail and recreational outlets as
270 a proxy for population adherence to NPIs, in the absence of high resolution temporal data specific to NPI
271 adherence.

272 Future research could further explore the strategy of using the leading eigenvector of the next generation
273 matrix to tailor vaccination strategies to specific populations. Data on contact matrices specific to country,
274 age and location are increasingly available (27). Digital data sources such as from bluetooth-enabled devices
275 also show promise to enhance our understanding of population contact patterns (30). We should take
276 advantage of these data sources to optimize vaccination policies, for COVID-19 as well as other infectious

277 diseases.

278 To apply these results to COVID-19 pandemic mitigation, large-scale seroprevalence surveys before the
279 onset of vaccination could ascertain the level of a population's natural immunity. In populations where
280 SARS-CoV-2 seropositivity is high due to a Fall 2020 wave, vaccinating to interrupt transmission may
281 reduce COVID-19 mortality more effectively than targeting vulnerable groups. We also conclude that more
282 research with different types of models is urgently needed to evaluate how best to prioritise COVID-19
283 vaccination.

284 **Contributors.** MA and CTB conceived of the study. PJ analysed the model. All authors contributed to
285 study design and wrote the manuscript.

286 **Declaration of interests.** We declare no competing interests.

287 **Data sharing.** All empirical data used in this analysis are publicly available. The model simulation code is
288 available from co-authors upon request.

289 **Acknowledgement.** This research was supported by research grants from the Natural Sciences and Engi-
290 neering Research Council of Canada (MA, CTB), and the Ontario Ministry of Colleges and Universities
291 (MA, CTB).

292 References

- 293 1. IF Miller, AD Becker, BT Grenfell, CJE Metcalf, Disease and healthcare burden of COVID-19 in the
294 United States. *Nat. Medicine* **26**, 1212–1217 (2020).
- 295 2. SC Anderson, et al., Estimating the impact of COVID-19 control measures using a bayesian model of
296 physical distancing. *medRxiv* (2020).
- 297 3. CM Peak, et al., Individual quarantine versus active monitoring of contacts for the mitigation of COVID-
298 19: a modelling study. *The Lancet Infect. Dis.* (2020).
- 299 4. AR Tuite, DN Fisman, AL Greer, Mathematical modelling of COVID-19 transmission and mitigation
300 strategies in the population of ontario, canada. *CMAJ* **192**, E497–E505 (2020).
- 301 5. N Lurie, M Saville, R Hatchett, J Halton, Developing COVID-19 vaccines at pandemic speed. *New*
302 *Engl. J. Medicine* **382**, 1969–1973 (2020).
- 303 6. KM Bubar, et al., Model-informed COVID-19 vaccine prioritization strategies by age and serostatus.
304 *medRxiv* (2020).
- 305 7. JH Buckner, GH Chowell, MR Springborn, Optimal dynamic prioritization of scarce COVID-19 vaccines.
306 *medRxiv* (2020).
- 307 8. J Hilton, MJ Keeling, Estimation of country-level basic reproductive ratios for novel coronavirus
308 (COVID-19) using synthetic contact matrices. *medRxiv* (2020).
- 309 9. RM Anderson, B Anderson, RM May, *Infectious diseases of humans: dynamics and control.* (Oxford
310 university press), (1992).
- 311 10. J Dushoff, et al., Vaccinating to protect a vulnerable subpopulation. *PLoS Med* **4**, e174 (2007).
- 312 11. Australian Government, Department of Health, Australian influenza surveillance report. **2(20 April**
313 **to 3 May 2020)** (2020).
- 314 12. S Bansal, B Pourbohloul, LA Meyers, A comparative analysis of influenza vaccination programs. *PLoS*
315 *Med* **3**, e387 (2006).
- 316 13. JS Brownstein, KP Kleinman, KD Mandl, Identifying pediatric age groups for influenza vaccination
317 using a real-time regional surveillance system. *Am. J. Epidemiol.* **162**, 686–693 (2005).
- 318 14. SA Pedro, et al., Conditions for a second wave of COVID-19 due to interactions between disease
319 dynamics and social processes. *medRxiv* (2020).
- 320 15. TC Reluga, Game theory of social distancing in response to an epidemic. *PLoS Comput. Biol* **6**,
321 e1000793 (2010).

- 322 16. M Salathé, S Bonhoeffer, The effect of opinion clustering on disease outbreaks. *J. The Royal Soc.*
323 *Interface* **5**, 1505–1508 (2008).
- 324 17. S Funk, E Gilad, C Watkins, VA Jansen, The spread of awareness and its impact on epidemic outbreaks.
325 *Proc. Natl. Acad. Sci.* **106**, 6872–6877 (2009).
- 326 18. F Verelst, L Willem, P Beutels, Behavioural change models for infectious disease transmission: a
327 systematic review (2010–2015). *J. The Royal Soc. Interface* **13**, 20160820 (2016).
- 328 19. S Funk, M Salathé, VA Jansen, Modelling the influence of human behaviour on the spread of infectious
329 diseases: a review. *J. Royal Soc. Interface* **7**, 1247–1256 (2010).
- 330 20. CT Bauch, Imitation dynamics predict vaccinating behaviour. *Proc. Royal Soc. B: Biol. Sci.* **272**,
331 1669–1675 (2005).
- 332 21. C Innes, M Anand, CT Bauch, The impact of human-environment interactions on the stability of
333 forest-grassland mosaic ecosystems. *Sci. reports* **3**, 1–10 (2013).
- 334 22. TM Bury, CT Bauch, M Anand, Charting pathways to climate change mitigation in a coupled socio-
335 climate model. *PLoS computational biology* **15**, e1007000 (2019).
- 336 23. MA Amaral, MM de Oliveira, MA Javarone, An epidemiological model with voluntary quarantine
337 strategies governed by evolutionary game dynamics. *arXiv preprint arXiv:2008.05979* (2020).
- 338 24. S Zhao, et al., Imitation dynamics in the mitigation of the novel coronavirus disease (COVID-19)
339 outbreak in wuhan, china from 2019 to 2020. *Annals Transl. Medicine* **8** (2020).
- 340 25. M Alam, KA Kabir, J Tanimoto, Based on mathematical epidemiology and evolutionary game theory,
341 which is more effective: quarantine or isolation policy? *J. Stat. Mech. Theory Exp.* **2020**, 033502 (2020).
- 342 26. T Wise, TD Zbozinek, G Micheleni, CC Hagan, , et al., Changes in risk perception and protective
343 behavior during the first week of the COVID-19 pandemic in the united states. (2020).
- 344 27. K Prem, AR Cook, M Jit, Projecting social contact matrices in 152 countries using contact surveys and
345 demographic data. *PLoS computational biology* **13**, e1005697 (2017).
- 346 28. R Sigdel, M Anand, CT Bauch, Convergence of socio-ecological dynamics in disparate ecological systems
347 under strong coupling to human social systems. *Theor. Ecol.* **12**, 285–296 (2019).
- 348 29. Organisation for Economic Co-operation and Development, Oecd intensive care bed capacity,
349 <https://www.oecd.org/coronavirus/en/data-insights/intensive-care-beds-capacity>, accessed 25 septem-
350 ber 2020 (2020).
- 351 30. M Salathe, et al., Digital epidemiology. *PLoS Comput. Biol* **8**, e1002616 (2012).

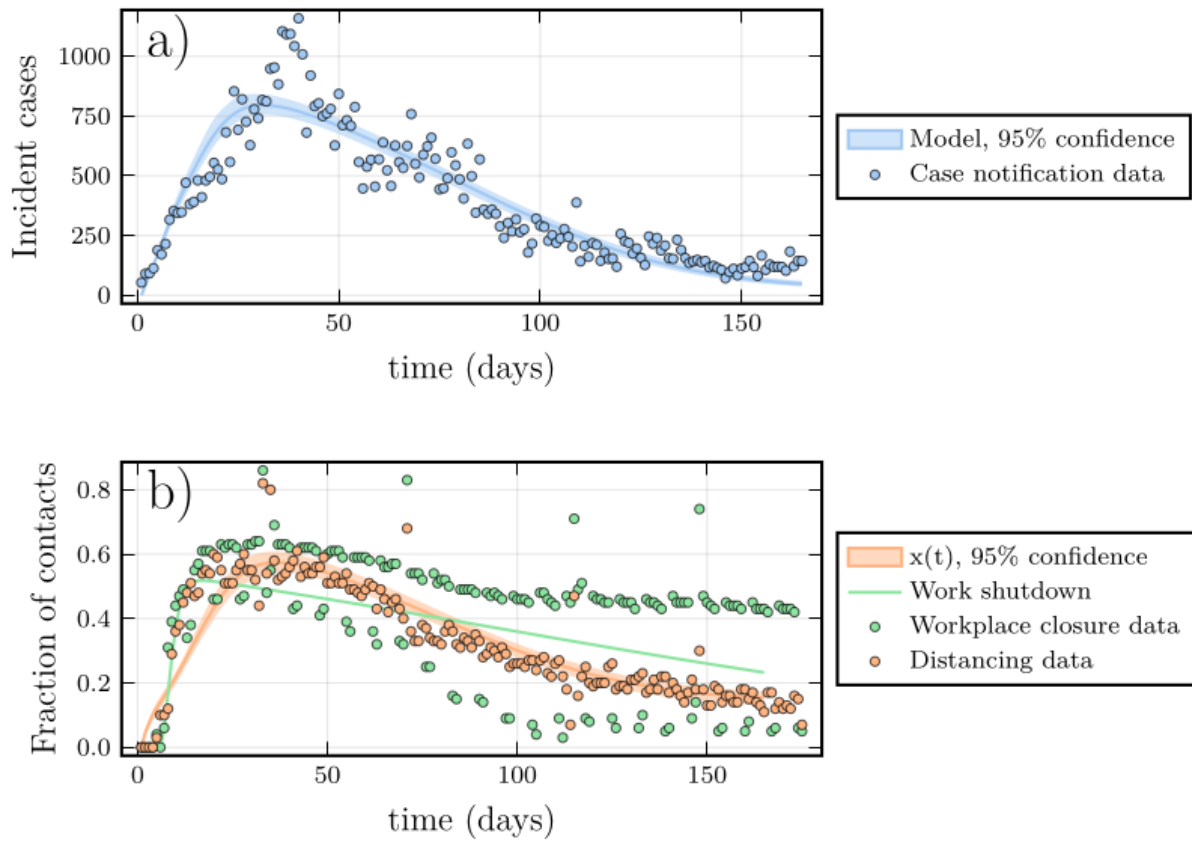


Fig. 1. A proxy for adherence to NPIs mirrors COVID-19 case reports in both data and model. (a) COVID-19 cases by date of report in Ontario (circles) and ascertained cases from best fitting model (lines). (b) Percentage change from baseline in time spent at retail and recreation destinations (orange circles) and at workplaces (green circles) from Google mobility data, and proportion of the population x practicing social distancing (orange line) and workplace shutdown curve (green line) from fitted model. See Supplementary Appendix for details on methods and data.

Vaccination begins on Jul 1, 2021, shutdown at 200.0% of first wave

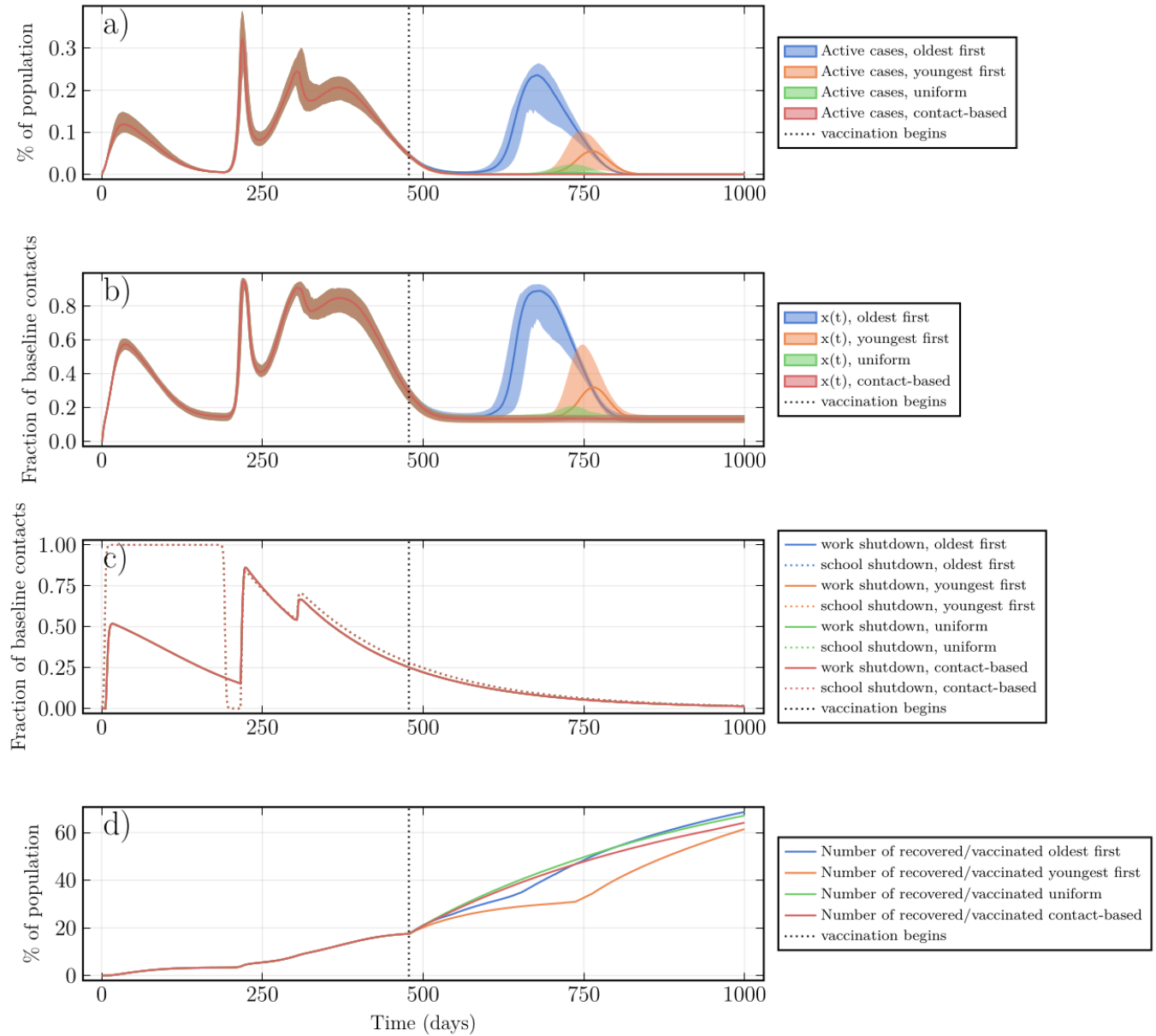


Fig. 2. Social and epidemic dynamics interact to determine pandemic waves and vaccine strategy effectiveness. (a) Active ascertained COVID-19 cases, (b) proportion x of the population practicing NPIs, (c) intensity of school and workplace closure (note that curves for different vaccination strategies overlap), and (d) percentage of population with natural or vaccine-derived immunity versus time. $T = 2.0$, $\psi_0 = 1.5\%$ per week, July 2021 vaccine availability, other parameters in Table S1.

It is made available under a [CC-BY-NC-ND 4.0 International license](https://creativecommons.org/licenses/by-nc-nd/4.0/).

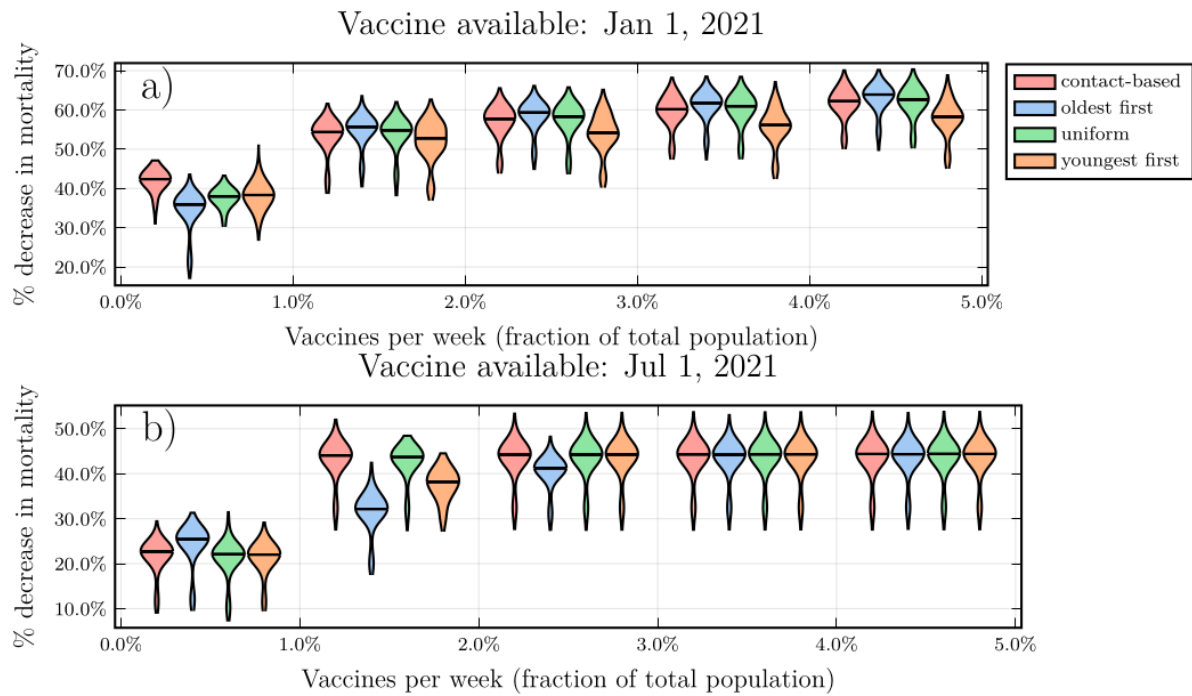


Fig. 3. A later start to vaccination favours transmission-interrupting vaccine strategies. Violin plots of the percent reduction in mortality under the four vaccine strategies, relative to no vaccination, as a function of the vaccination rate ψ_0 , for (a) January and (b) July 2021 availability. Horizontal lines represent median values of posterior model projections. Shutdown threshold $T = 2.0$ and other parameter values in Table S1.

It is made available under a [CC-BY-NC-ND 4.0 International license](https://creativecommons.org/licenses/by-nc-nd/4.0/).

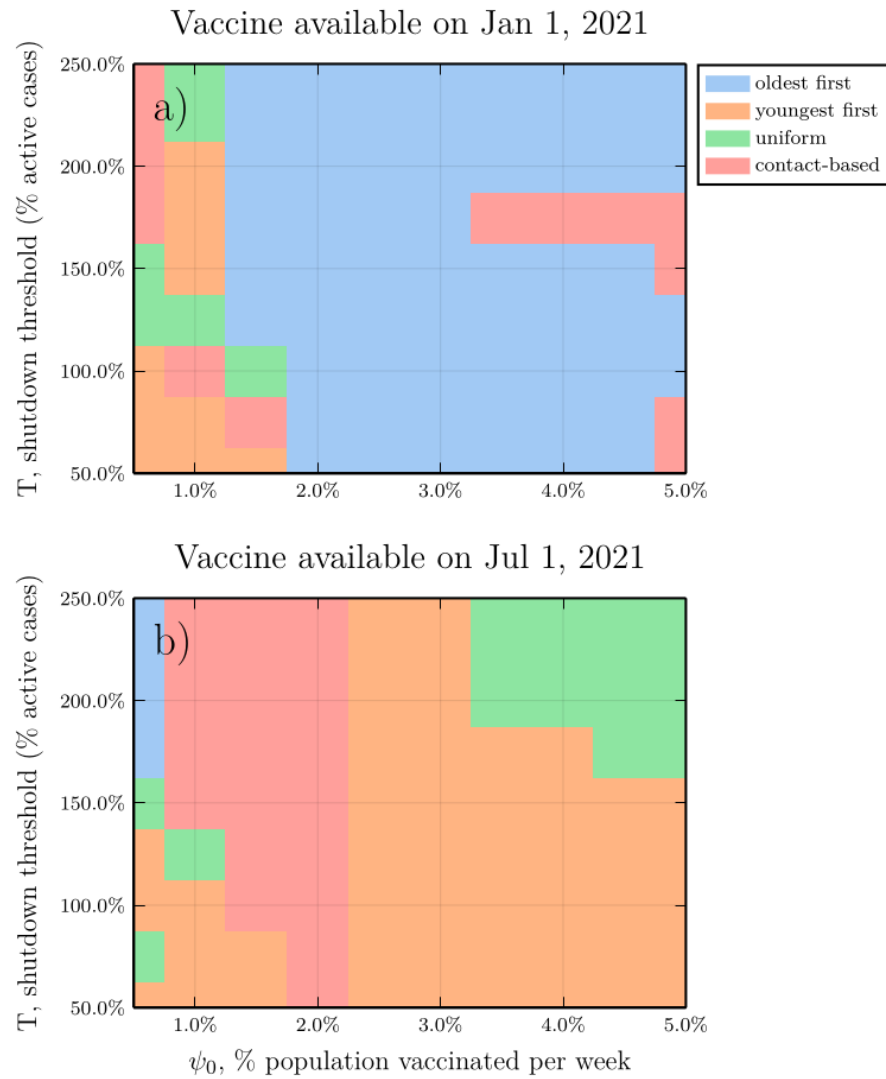


Fig. 4. Parameter planes showing best strategy as a function of shutdown threshold T and vaccination rate ψ_0 . Each parameter combination on the plane is colour-coded according to which of the four strategies reduced mortality most effectively in the largest number of model realizations, for (a) January and (b) July 2021 availability. Other parameter values in Table S1.

It is made available under a [CC-BY-NC-ND 4.0 International license](https://creativecommons.org/licenses/by-nc-nd/4.0/).

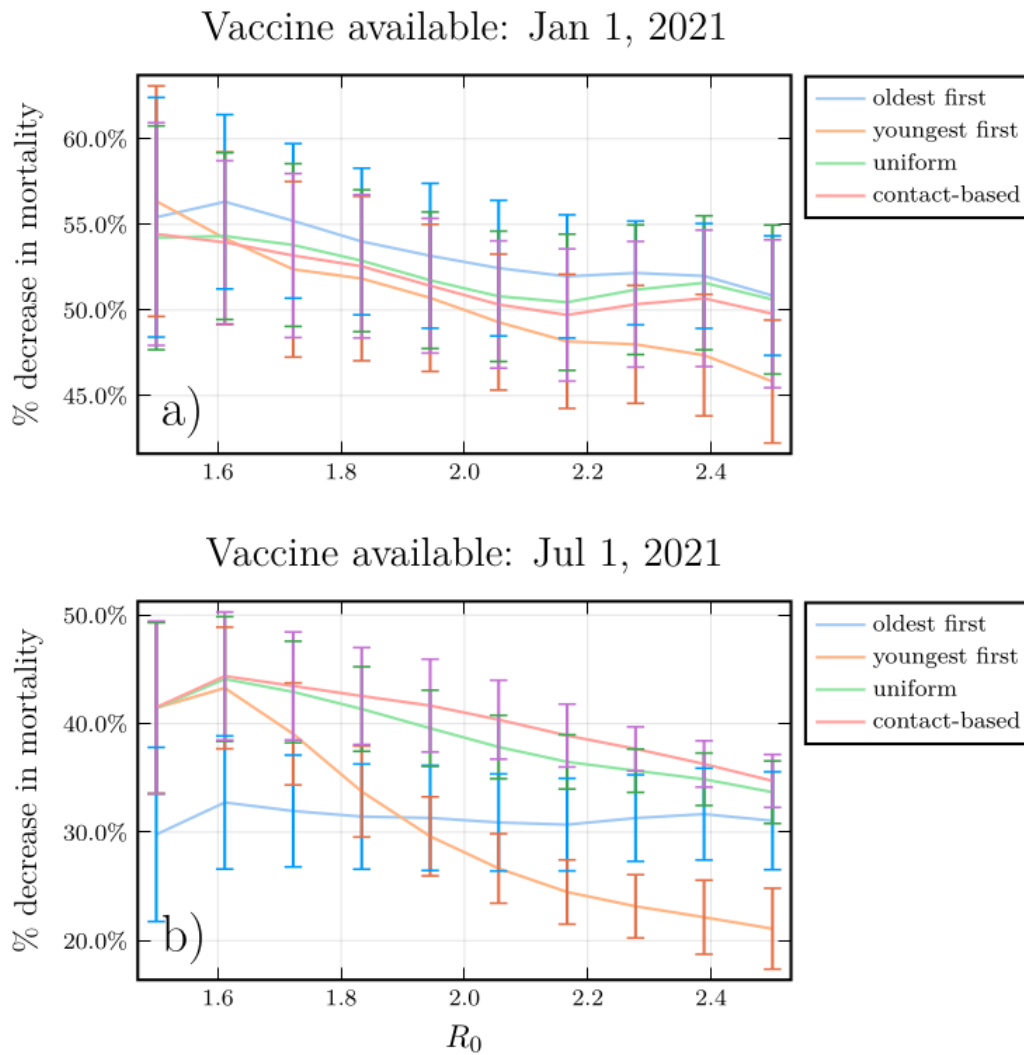


Fig. 5. A higher R_0 diminishes the relative advantage of transmission-interrupting vaccination strategies. Median and standard deviation of the percent reduction in mortality under the four vaccine strategies, relative to no vaccination, as a function of the basic reproduction number R_0 , for (a) January and (b) July 2021 availability. Shutdown threshold $T = 2.0$, vaccination rate $\psi_0 = 1.5\%$ per week, and other parameter values in Table S1.

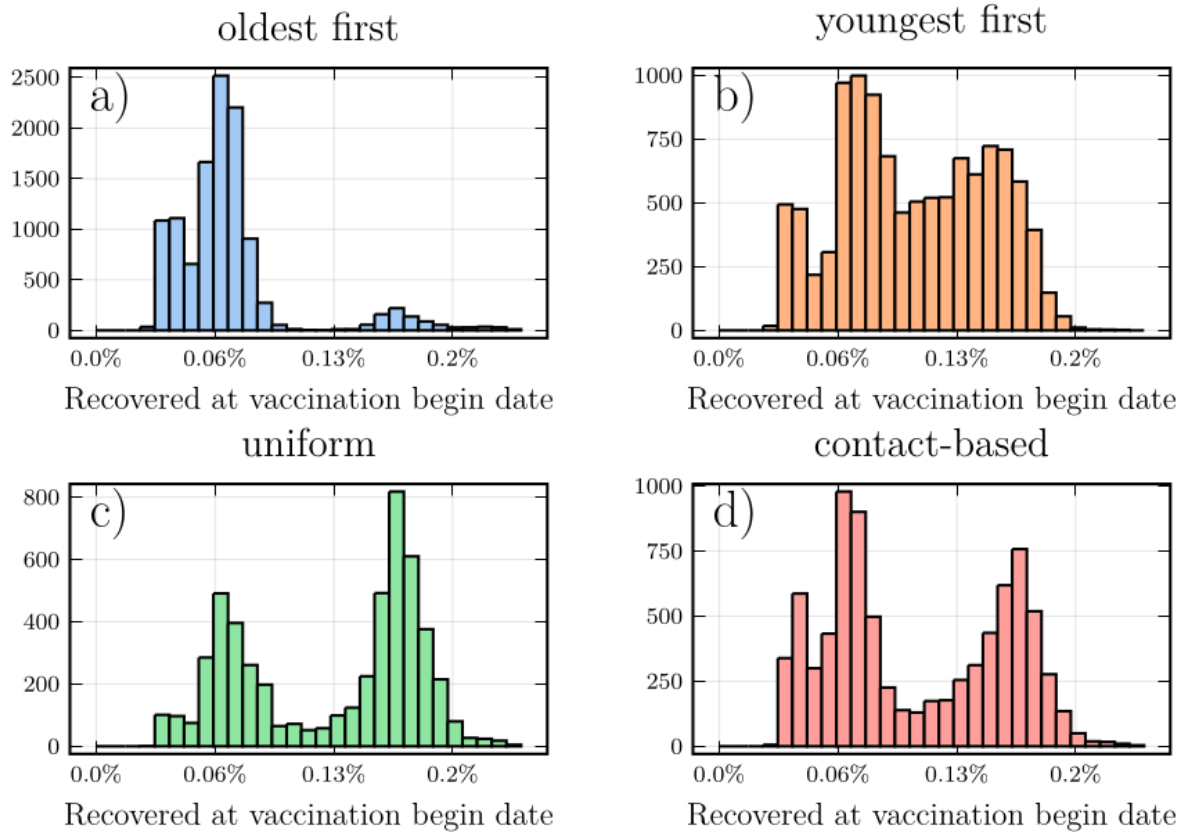


Fig. 6. Higher rates of pre-existing natural immunity make transmission-interrupting strategies more effective. Frequency histogram of the percentage of the population with natural immunity for each strategy, taken from simulations where that strategy reduced mortality most effectively, for (a) oldest first, (b) youngest first, (c) uniform, and (d) contact-based strategies. Parameter values in Table S1.